Soil Dynamics and Earthquake Engineering 115 (2018) 217–224

Contents lists available at ScienceDirect

Soil Dynamics and Earthquake Engineering

journal homepage: www.elsevier.com/locate/soildyn

Influence of size disparity on small-strain shear modulus of sand-fines mixtures

Xin Liu[a,*,1], Jun Yang[b]

[a] Department of Geology Engineering, Chang'an University, Xi'an, China
[b] Department of Civil Engineering, The University of Hong Kong, Hong Kong, China

ARTICLE INFO

Keywords:
Shear modulus
Sand-fines mixtures
Fines content
Particle size disparity

ABSTRACT

Characterizing the small-strain shear modulus (G_0) of sand with fines is of importance in geotechnical applications since natural sand is usually not clean but contains a certain amount of fines. This paper presents an experimental study to investigate G_0 values of several sand-fines mixtures, formed by mixing clean quartz sands of different sizes with crushed silica fines of varying quantity. Focus of the study is on the possible interplay between the influence of particle size disparity and the influence of fines contents for which current understanding is not adequate. By defining the particle size disparity as D_{50}/d_{50}, where D_{50} is the mean size of base sand and d_{50} is the mean size of fines, a critical range of size disparity is found to be approximately between 4 and 7. When the size disparity is smaller than 4, the role of fines is manifested mainly by fines content; when the size disparity is beyond 7, the contribution of fines to the load transfer gradually becomes negligible because in this case fine grains tend to roll into the voids. A new concept, referred to as combined size disparity, is proposed to capture the influence of fines content and the influence of size disparity in a collective manner. By adopting this concept, an empirical relationship is proposed for estimating G_0 values of sand-fines mixtures. The predictive performance of the relationship is then examined using literature data and a reasonably good agreement between prediction and measurement is obtained.

1. Introduction

Sand-fines mixtures are often gap-graded in the sense that grains within a certain range of size are missing in comparison with conventional granular soils of continuous grading. When studying the various behavior of sand-fines mixtures, the quantity of fines (i.e. fines content) is usually regarded as a key factor [1–3]. In recent years, there is a growing interest in the small-strain shear modulus (G_0) of sand-fines mixtures. (e.g., [4–8]). While a general trend has been found that the G_0 value decreases with fines content, the reduction is not always identical among different sand-fines mixtures. For instance, at similar void ratios, Salgado et al. [6] observed a reduction of G_0 value as much as 60% for Ottawa sand mixed with 15% of silica fines, whereas a much less reduction (~ 17%) was reported by Chien and Oh [4] for a reclaimed sandy soil with 20% fines content. Moreover, a recent finding from Yang and Liu [8] shows that the state dependence of G_0 of sand-fines mixtures can be characterized in a unified way for a range of fines content by using the concept of state parameter [9]. In the framework of critical state soil mechanics, the state parameter is a measure of soil state with reference to the critical state locus in the compression space. It is worth noting that the critical state locus of sand-fines mixtures depends not only on fines content but also on grain characteristics [10–12]. This leads to an important implication that the influence of fines on G_0 cannot be fully characterized by using fines content. The significant differences in the reduction of G_0 at a given fines content, as discussed above, are certainly attributed to factors other than fines content.

In this paper, we propose that the size disparity ratio, defined as the ratio between mean particle sizes of coarse and fine grains, is a major factor for the mechanical property of sand-fines mixtures. Experimental data yielded from a specifically designed testing program on the small-strain shear modulus of several different sand-fines mixtures are presented and analyzed. The aim of the study is to investigate the influence of size disparity along with the influence of fines content. Particular effort is made is to elucidate the possible coupling of these two factors on G_0.

* Corresponding author.
E-mail address: xliu67@chd.edu.cn (X. Liu).
[1] Formerly of The University of Hong Kong.

https://doi.org/10.1016/j.soildyn.2018.08.011
Received 24 February 2018; Received in revised form 20 June 2018; Accepted 9 August 2018
Available online 01 September 2018
0267-7261/

Notation

A	coefficient in Eq. (2)
C_u	coefficient of uniformity
d_{50}	mean size of fine grain
D_{50}	mean size of coarse grain
D_{com}	combined particle size
e	void ratio
e_s	skeleton void ratio
e^*	equivalent granular void ratio
F_c	fines content
$F(e)$	void ratio function
G_0	small-strain shear modulus
n	stress exponent
P_a	reference stress
Γ_{com}	combined size disparity
σ'	mean effective stress

2. Experimental program

2.1. Test materials

Three quartz sands, namely Toyoura sand, Fujian sand C, and Fujian sand D, were used as the base sand in the laboratory tests. Table 1 gives the basic physical properties of each base sand, and the microscopy images of these sands are presented in Fig. 1. Clearly all three base sands were uniformly graded with sub-rounded grains. In this connection, the influence on G_0 due to the difference of particle grading [13] and particle shape [14] is considered insignificant in the present study. To produce a sequence of mixtures of being sand dominant, crushed silica fines (less than 63 μm) of varying percentage (0%, 5%, 10%) were added to each base sand. For simplicity abbreviations were adopted for each mixture in the analysis; for example, TSS stands for mixtures with Toyoura sand as the base sand and FSS-C stands for mixtures with Fujian sand C as the base sand. Fines content is given as a number inside parentheses; for example FSS-D(5) represents Fujian sand D mixed with 5% silica fines. It is worth noting that these base sands were chosen such that a set of gap-graded sands of nearly parallel grading with a range of particle size disparities were produced. To make this point clear, the particle size distribution curves of each test material are plotted in Fig. 2. It can be seen that the TSS mixtures exhibit the smallest particle size disparity whereas the FSS-D mixtures have the greatest size disparity.

2.2. Apparatus and test procedure

The small-strain shear modulus (G_0) was determined using a resonant column (RC) apparatus in the bottom-fixed and top-free configuration. The device can accommodate a cylindrical specimen of 50 mm in diameter and 100 mm in height, with an air-filled cell pressure up to 1 MPa. By applying acceleration through exciters mounted on the top of specimen, an overall response of the specimen can be recorded. An internal LVDT of high-resolution can measure the specimen's deformation with time. The strain level involved in all tests was found in the order of 10^{-5} or below. Readers may refer to Yang and Gu [15] for more details about the apparatus.

All specimens were prepared by the moist tamping method [16] in conjunction with the under-compaction technique (i.e., use 1% of under-compaction ratio) [17] and the global void ratio (e) was used as a target parameter. This method was chosen because it can produce a wide range of void ratios and has the advantage of preventing segregation of fine and coarse grains. All specimens were tested under saturated conditions. Carbon dioxide was used to circulate through the specimen, which was then followed by flushing the specimen with deaired water. To further increase the degree of saturation, back pressure saturation (i.e., 350 kPa) was applied and a B-value greater than 0.95 was ensured. Isotropic confining stress was applied in a stepwise manner on the same specimen, and when bringing the specimen to a specific effective stress level, consolidation of 30 min was adopted so that the reading of LVDT became stable and the volume change of the specimen was recorded. The testing series are listed in Table 2. For completeness, testing series of Toyoura sand mixtures can be found in Yang and Liu [8].

3. Test results and discussions

3.1. Effects of size disparity and fines content on G_0

In Fig. 3 the G_0 values of all base sands are compared. It is clear that void ratio and confining stress are two important factors affecting G_0. For a given confining stress G_0 increases with decreasing void ratio, whereas for a given void ratio G_0 decreases with deceasing confining stress. Under the same confining stress and the same void ratio, the three base sands exhibit similar G_0 values. Recalling that these base sands are of parallel grading (C_u = 1.4–1.5) with different mean particle size (D_{50}), the above observation indicates that mean particle size is not the main factor controlling G_0, in agreement with the finding of Yang and Gu [15] derived from laboratory experiments on glass beads.

In Fig. 4 measured G_0 values for gap-graded sands with fines content of 5% and 10% are plotted as a function of void ratio. It is interesting to note that, under otherwise similar conditions, the influence of fines content on G_0 is differing for different base sand. For example at $e = 0.8$ and σ' = 100 kPa, the G_0 value of TSS(5) is about 28% higher than that of FSS-C(5) and becomes one-fold greater than that of FSS-D(5). More pronounced distinction can be seen in Fig. 4(b) for specimens with higher fines content. While the differences between FSS-C(10) and FSS-D(10) appear to reduce, the G_0 values of TSS(10) remain markedly high despite having greater void ratios.

To remove the influence of void ratio (e), a common method was adopted by normalizing G_0 with a void ratio function as follows [18]. Note that $a = 2.17$ was adopted here based on the comprehensive investigation by Iwasaki and Tatsuoka [19].

$$F(e) = \frac{(a - e)^2}{1 + e} \tag{1}$$

In Fig. 5 the void ratio corrected G_0 values are plotted as a function of effective stress (σ') that is also normalized by a reference stress (i.e., P_a = 98kPa). The stress dependence is evident from the plots and it can be described using Eq. (2). For each mixture, a high coefficient of determination was obtained (R^2 greater than 0.97).

$$\frac{G_0}{F(e)} = A\left(\frac{\sigma'}{P_a}\right)^n \tag{2}$$

It is worth noting that the void ratio corrected G_0 is the greatest for TSS mixture and is the smallest for FSS-D mixture. The data in Fig. 5

Table 1
Physical properties of tested materials.

Properties	Toyoura sand	Fujian sand-C	Fujian sand-D	Crushed Silica	Crushed glass bead
G_s	2.65	2.65	2.65	2.64	2.65
D_{10} (μm)	166	282	658	27.5	9.1
D_{50} (μm)	216	397	890	54	31.8
D_{60} (μm)	231	432	948	60	37.8
C_u	1.39	1.53	1.44	2.18	4.15

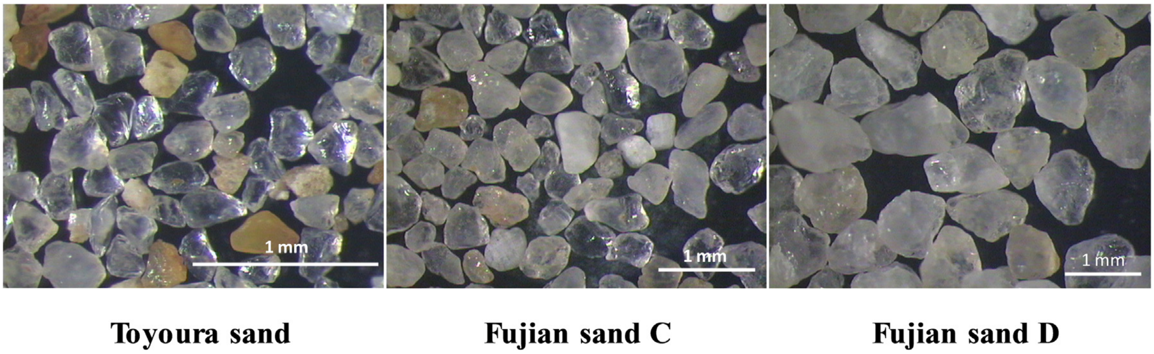

Fig. 1. Microscopic images of base sands.

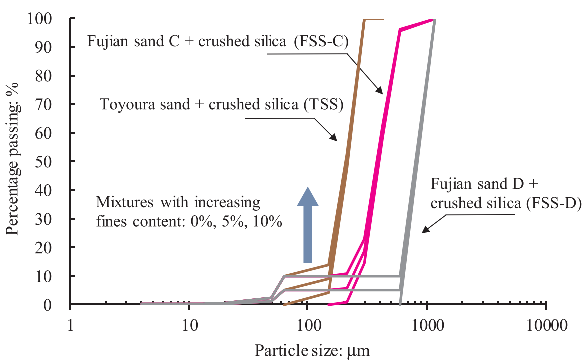

Fig. 2. Particle size distribution curves of tested materials.

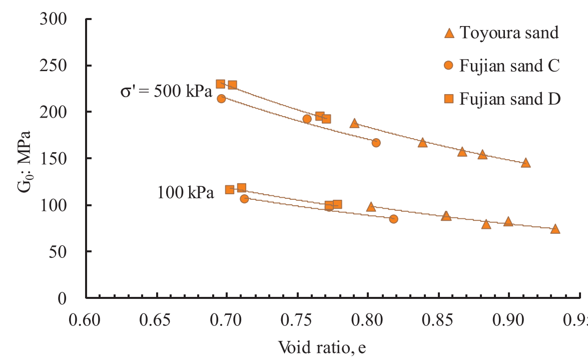

Fig. 3. Variation of G_0 values with void ratio at different stress levels for base sand.

provides solid evidence for the marked influence of particle size disparity. To view this influence in a different way, the particle size disparities of the mixtures are compared in a bar chart along with the best-fit stiffness parameters (A and n) obtained from Eq. (2). It is clear that the FSS-D mixture has the largest particle size disparity (D_{50}/d_{50} = 16.51), which is about 4 times greater than that of the TSS mixture. Besides, the A value of FSS-D(10) reduces as much as 28% when compared with FSS-D(5), and accordingly the n value increases from 0.53 to 0.59.

Given the above observations, a question arises as to whether a change of fines content induce the same impact on G_0 for mixtures of different base sands. To address this question, the best-fit parameters are plotted as a function of fines content in Fig. 7. It is interesting to note that, while there is a general trend that the A value decreases with fines content, the amount of reduction is controlled by particle size disparity. For instance, the reduction is prominent for FSS-D that has highest particle size disparity. On the other hand, the n value increases with fines content and it is apparently greater than 1/3 — the theoretically derived exponent for packings of uniform spheres [20]. These observations suggest that there is an interplay between the influence of fines content and the influence of particle size disparity and the two

Table 2
Summary of testing series.

Specimen	State 1 (e, σ')	State 2 (e, σ')	State 3 (e, σ')	State 4 (e, σ')	State 5 (e, σ')
Fujian sand C (F_c = 0%)	(0.773,100)	(0.767,200)	(0.763,300)	(0.760,400)	(0.757,500)
	(0.713,100)	(0.707,200)	(0.703,300)	(0.700,400)	(0.697,500)
	(0.818,100)	(0.814,200)	–	–	(0.806,500)
FSS-C (F_c = 5%)	(0.713,100)	(0.708,200)	(0.704,300)	(0.700,400)	(0.698,500)
	(0.770,100)	(0.763,200)	(0.758,300)	(0.754,400)	(0.750,500)
	(0.803,100)	(0.799,200)	–	–	(0.790,500)
	(0.822,100)	(0.817,200)	–	–	(0.806,500)
FSS-C (FC = 10%)	(0.706,100)	(0.699,200)	(0.694,300)	(0.690,400)	(0.687,500)
	(0.707,100)	(0.700,200)	(0.694,300)	(0.690,400)	(0.685,500)
	(0.766,100)	(0.756,200)	(0.748,300)	(0.742,400)	(0.736,500)
Fujian sand D (F_c = 0%)	(0.702,100)	(0.700,200)	(0.699,300)	(0.697,400)	(0.696,500)
	(0.711,100)	(0.709,200)	(0.707,300)	(0.705,400)	(0.704,500)
	(0.773,100)	(0.771,200)	(0.769,300)	(0.767,400)	(0.766,500)
	(0.778,100)	(0.776,200)	(0.774,300)	(0.773,400)	(0.771,500)
FSS-D (F_c = 5%)	(0.703,100)	(0.700,200)	(0.698,300)	(0.696,400)	(0.694,500)
	(0.774,100)	(0.769,200)	(0.766,300)	(0.762,400)	(0.759,500)
	(0.814,100)	(0.803,200)	(0.796,300)	(0.788,400)	(0.783,500)
FSS-D (F_c = 10%)	(0.707,100)	(0.701,200)	(0.697,300)	(0.693,400)	(0.689,500)
	(0.766,100)	(0.759,200)	(0.753,300)	(0.745,400)	(0.738,500)
	(0.806,100)	(0.785,200)	(0.770,300)	(0.758,400)	(0.748,500)

Note: e = void ratio; σ' = effective confining stress (kPa); F_c = fines content.

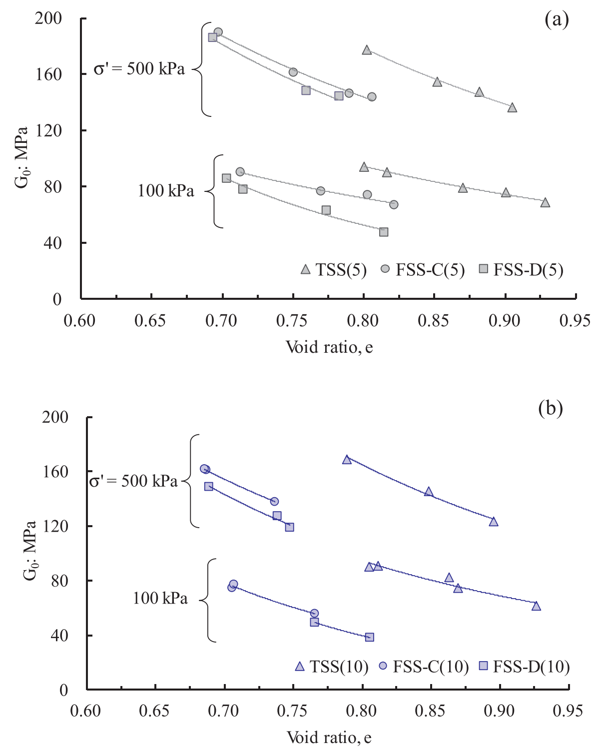

Fig. 4. Variation of G_0 values with void ratio at different stress levels for: (a) F_c = 5%; (b) F_c = 10%.

factors should be collectively accounted for.

3.2. Critical range of size disparity

To characterize the behavior of sand-fines mixtures, a concept known as skeleton void ratio (e_s) was often adopted to facilitate comparisons between the fines content. As a matter of fact, e_s can be regarded as a special case of the so-called equivalent granular void ratio (e^*) [21,22] with the hypothesis that all fine grains reside in the void space with little contribution to the load transfer [23–25]. An expression of this concept is presented in the following:

$$e_s = \frac{e + F_c}{1 - F_c} \tag{3}$$

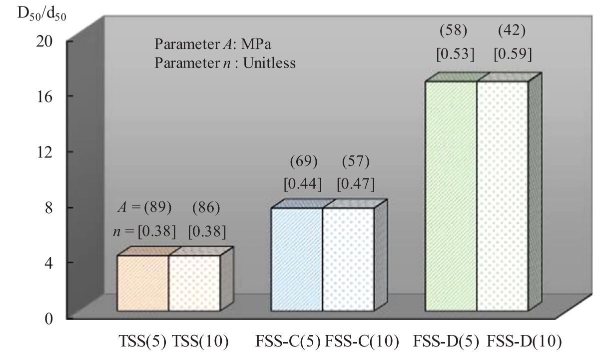

Fig. 6. Size disparity ratios of sand-fines mixtures.

where F_c is fines content in decimal. The above expression suggests that the skeleton void ratio increases with fines content. In Fig. 8 the G_0 values of gap-graded sands with fines are plotted as a function of e_s. Interestingly, a unique trend of data emerges for FSS-C and FSS-D regardless of fines content, and this seems to suggest that the use of e_s is viable in accounting for the influence of fines. However, Toyoura sand mixtures apparently exhibit different trend lines: for a given skeleton void ratio, the specimen having greater fines content yields higher G_0 values. This means a beneficial effect of fines on G_0. For instance, as shown in this figure, at a skeleton void ratio around 0.98–0.99 and stress level of 500 kPa, the G_0 value of TSS(10) is about 30% higher than TSS(5). This result is against the general consensus that the effect of fines is detrimental on G_0 [4–8,26].

The discrepancy in Fig. 8 indicates that fines cannot be simply treated as voids but rather their role is highly complex and depends on size disparity. For TSS mixtures, the size disparity (D_{50}/d_{50}) is around 4 whereas for FSS-C mixtures the size disparity is around 7.4. It is postulated here that a critical range of size disparity is between 4 and 7 for sand-fines mixtures (sand dominant). When the size disparity is smaller than 4, the amount of fine grains cannot be simply replaced by voids and the role of fines in load transfer is manifested mainly by fines content. On the contrary, when the size disparity increases beyond 7, fine grains tend to roll into the voids and the contribution of fines to the load transfer gradually becomes negligible.

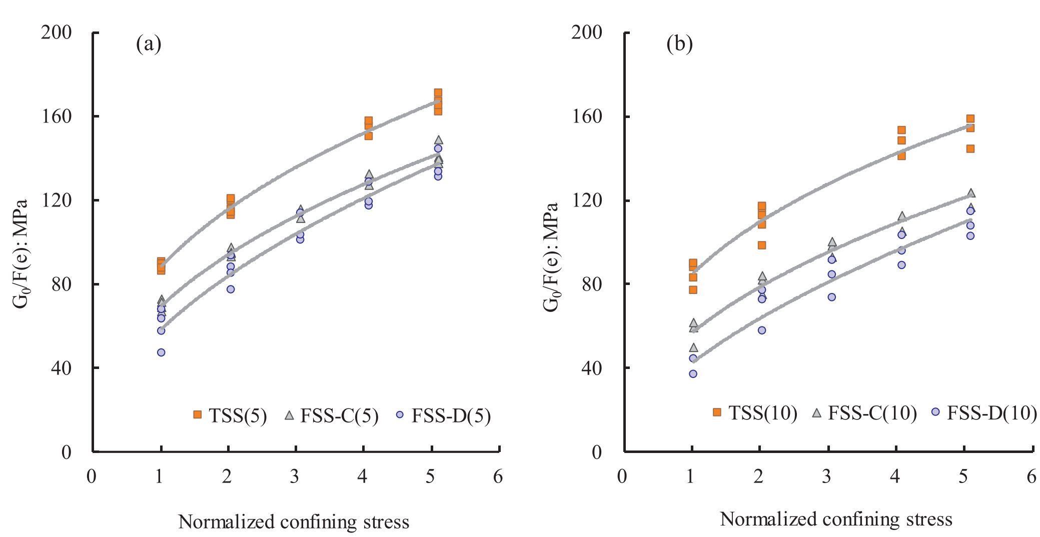

Fig. 5. Void ratio-corrected G_0 values as a function of normalized confining stress: (a) F_c = 5%; (b) F_c = 10%.

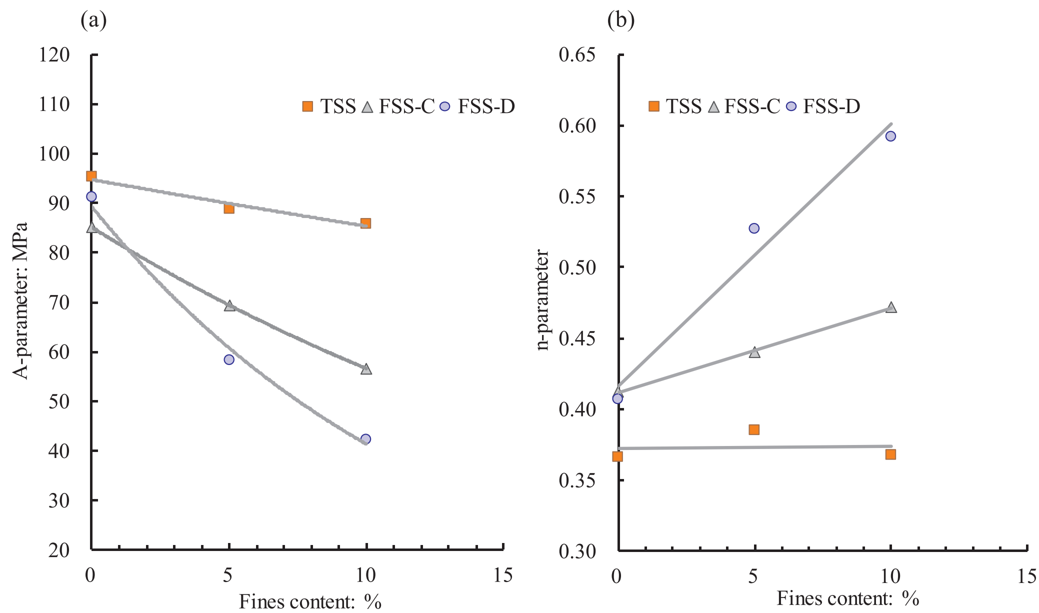

Fig. 7. Variation of stiffness parameters with fines content: (a) A parameter; (b) n parameter.

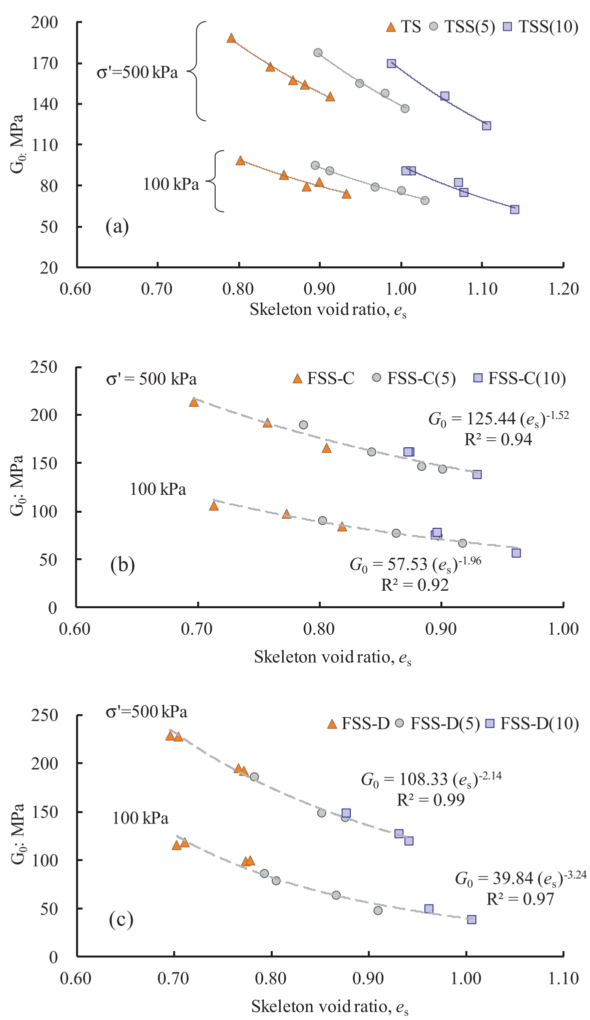

Fig. 8. Variation of G_0 values with skeleton void ratio: (a) TSS mixture; (b) FSS-C mixture; (c) FSS-D mixture.

4. Predictive model of G_0

4.1. Combined size disparity

To predict the G_0 values, in the above context, a routine method that only uses the fines content as an input parameter is apparently inadequate. As a desired complement, a new index namely combined particle size (D_{com}) is proposed in this study. The new term is similar with the combined roundness used by Yang and Wei [12] in that both aim to take account of the influencing factors for an overall evaluation. Accordingly, an expression of D_{com} is given in Eq. (4).

$$D_{com} = F_c(d_{50}) + (1 - F_c)D_{50} \tag{4}$$

where F_c is fines content in decimal; d_{50} and D_{50} represent the mean size of fine and coarse grains, respectively. Compared with the size disparity (Fig. 6), the combined particle size is more versatile as it also captures the influence of fines content. For instance, mixtures having greater fines content exhibit smaller D_{com} values. Note that for the sand dominated mixtures, the magnitude of D_{com} is mainly controlled by the mean size of coarse grains (D_{50}). In other words, the D_{com} values always fluctuate within a range near the value of D_{50}. Recalling the observations in Fig. 3 that the mean size of base sands has no effect on the G_0 values, in this connection, the above concept (D_{com}) needs further revision. The difference of D_{com} between the gap-graded sand and the clean sand is therefore adopted to rule out the influence of D_{50} and the relationship is presented in the following:

$$\Gamma_{com} = D_{com,0} - D_{com,F_c} \tag{5}$$

where Γ_{com} is the abbreviation of combined size disparity, $D_{com,Fc}$ is the combined particle size at any fines content, and it equals to the mean particle size of clean sand when the fines content is zero (i.e., $D_{com,0} = D_{50}$). In Fig. 9, this new term is compared in a bar-chart among different test materials. A notable feature as compared with Fig. 6 is that the Γ_{com} values increase with fines content. At a given fines content, on the other hand, specimens with large size disparity exhibit higher Γ_{com} values.

By using this concept, the conventional approach in Eq. (2) is modified, in which a ratio of small-strain shear modulus between the mixtures ($G_{0,\alpha}$) and the clean sand ($G_{0,\beta}$) is derived below:

$$\frac{G_{0,\alpha}}{G_{0,\beta}} = \frac{A_\alpha}{A_\beta}\left(\frac{\sigma'}{P_a}\right)^{n_\alpha - n_\beta} \tag{6}$$

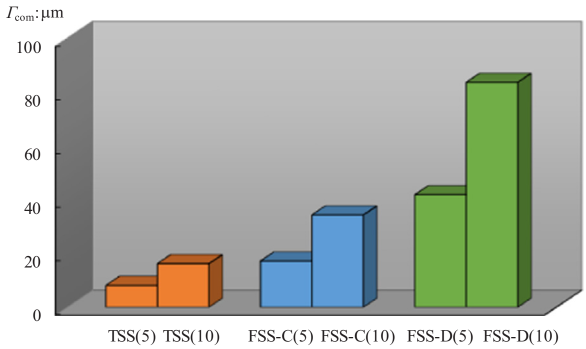

Fig. 9. Values of combined size disparity of sand-fines mixtures.

where A_α and n_α are the best-fit parameters of mixtures at a certain fines content (i.e., Eq. (2)); A_β and n_β are the best-fit parameters of clean sand. Compared with a gap-graded sand, the determination of G_0 values in a clean sand is straightforward. By using Eq. (6), the G_0 values of a gap-graded sand are therefore estimated with a premise of knowing that for the clean sand. In Fig. 10, the best-fit parameters in Eq. (6) are readily plotted as a function of combined size disparity. In each plot, the trend lines can be described respectively as follows:

$$\frac{A_\alpha}{A_\beta} = \exp\left(-0.01\Gamma_{com}\right) \tag{7}$$

$$n_\alpha - n_\beta = 0.002\Gamma_{com} \tag{8}$$

Note that Eq. (7) is the natural exponential function with $e = 2.71$. At $\Gamma_{com} = 0$, the best-fit parameters of mixtures remain the same as clean sand. By combining the Eqs. (6), (7), and (8), the G_0 values of test materials were estimated. As an example, the predicted G_0 values of mixtures are compared with the measured ones in Fig. 11, showing a reasonably good agreement.

4.2. Validation

In a rigorous manner, practicability of the proposed method is an interesting concern. It is thereby highly desired to evaluate the proposed equations using extra groups of data. For this reason, resonant column tests were also carried out on the mixtures with crushed glass beads fines (CGB) following the same test procedures as aforementioned. To facilitate the comparison, particle size distribution curve of the crushed glass beads fines is plotted in Fig. 12 along with the crushed silica fines (CS) and the physical properties are also given in Table 1. It is clear that the mean particle size of CGB is smaller than CS. Accordingly, the crushed glass beads mixtures exhibit higher particle size disparity than that of crushed silica mixtures. Also, noted from this figure, the microscopic images of the fine grains demonstrate quite similar particle characteristics. By using the empirical method proposed in the above context, the G_0 values of sand-fines mixture with glass beads fines are estimated. The predictions are compared with the measured ones from the RC test in Fig. 13. Here, one may concern about the observation that the G_0 values of the mixture with glass bead fines are slightly overestimated by using the proposed model. It can be explained when the influence of gradation has been taken into account (i.e., G_0 values decreases with C_u) [13,19]. Compared with the CGB fines ($C_u = 4.15$), the size distribution of the CS fines ($C_u = 2.18$) used in the predictive model is apparently more uniform (Table 1), rendering higher G_0 values from the model. Yet, it is still encouraging to see that in general the discrepancies in Fig. 13 are within a range of 10%, which is reasonably good as that in Fig. 11.

Furthermore, the predictive performance of empirical equations is also examined using experimental data from the literature (i.e., [4,6,27]). As shown in Fig. 14, the ratio of G_0 values between the mixtures and the clean sand is plotted as a function of the fines content. Note that the symbols in this figure indicates the experiment data from the literature, and the predicted values are described using the dash line. It is evident from this figure that the prediction using the empirical method agrees well with the experimental data from Huang et al. [27] and Chien and Oh [4] on the natural silty sand that is not gap-graded but in a continuous grading. When compared with the experimental results in Salgado et al. [6], however, the ratio of G_0 values is slightly overestimated. Bearing in mind that more rotund Ottawa sand was used in their study, the grain shape characteristics that often induces a strong influence on the G_0 values of clean sand [14] may add additional uncertainties in the prediction. Of course, further refinement and verification of the proposed empirical method is worthwhile when an enlarged data set becomes available.

5. Summary and conclusions

This paper presents an experimental study on the small-strain shear modulus (G_0) of gap-graded sand with fines, with particular effort to elucidate the coupled influence of fines content and particle size disparity. An empirical relationship has been developed for evaluating the G_0 values of sand-fines mixtures in a simple yet effective way. The main findings from this study are summarized as follows.

(a) At a given stress level the G_0 values of a set of uniformly graded clean quartz sands decrease in the same manner with void ratio. For these sands mixed with the same amount of fines, however, a distinct feature was found that the G_0 values of TSS mixture remain markedly higher than that of other two mixtures.
(b) Through a regression analysis using the Hardin's equation, the best-fit parameters (A and n) were obtained with high coefficients of determination. It was found that the parameter A decreases with

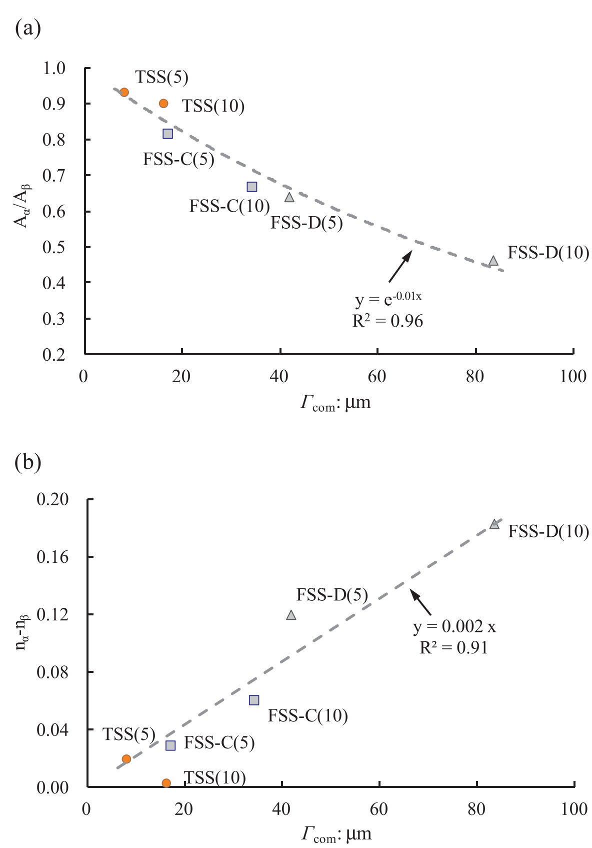

Fig. 10. Variation of stiffness parameters with combined size disparity: (a) A_α/A_β; (b) n_α -n_β.

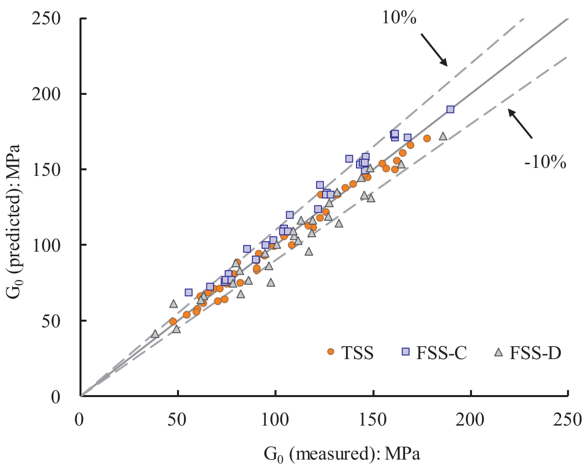

Fig. 11. Predicted and measured G_0 values of tested materials.

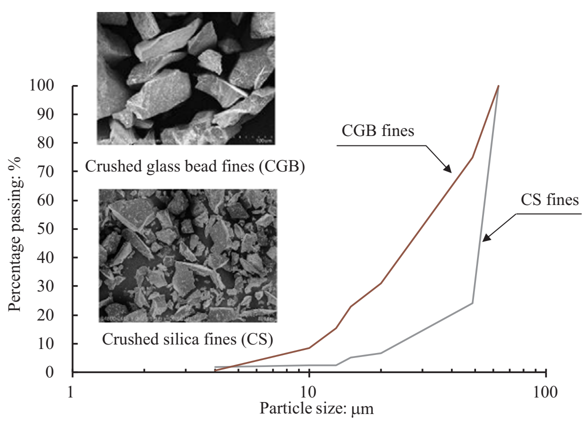

Fig. 12. Particle size distribution curves of fine grains.

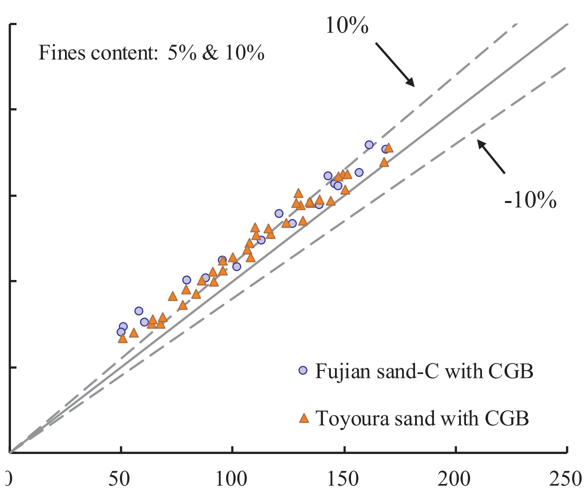

Fig. 13. Predicted and measured G_0 values of crushed glass beads (CGB) mixtures.

fines content, while the parameter n increases accordingly. Of more interest, the dependence becomes prominent for soils of higher particle size disparity.

(c) When comparisons of G_0 values were made using the concept of skeleton void ratio (e_s), a unique trend was found for the mixtures of FSS-C and FSS-D, implying that most fine grains play the role as voids in these mixtures. Under otherwise similar conditions, however, the TSS specimen of higher fines content yields greater G_0 values, which is in contradiction with the common understanding. Accordingly, a critical range of size disparity was defined, in such a way that it determines the role of fine grains in the load transfer.

(d) A new index, named combined size disparity, was proposed to take account of the coupled influence of fines content and particle size disparity, and empirical relationships on the basis of Hardin's formula were derived. Validations of the empirical relationships were carried out by comparing the predictions with extra data set as well as data from the literature, both yielding satisfied predictive performance.

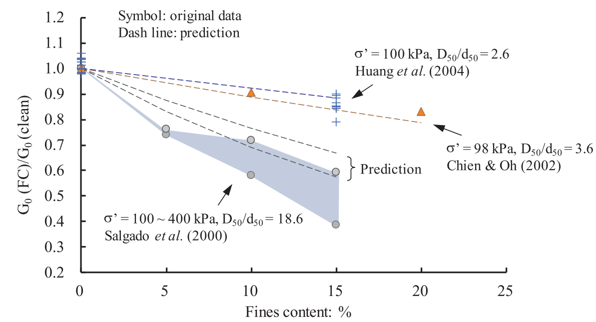

Fig. 14. Model prediction versus experimental data.

Acknowledgments

The financial support provided by the Research Grants Council of Hong Kong through the General Research Fund (No. 17250316) and by the University of Hong Kong through a matching fund to the NSFC's Academic Collaboration Award (No. 51428901) is gratefully acknowledged All experiments were conducted at the Soil Mechanics laboratory of the University of Hong Kong. Financial support provided by the National Natural Science Foundation of China (No. 51428901; 41807226) and by the Research Grants Council of Hong Kong (No. 17250316) is gratefully acknowledged.

References

[1] Thevanayagam S, Shenthan T, Mohan S, Liang J. Undrained fragility of clean sands, silty sands, and sandy silts. J Geotech Geoenviron Eng 2002;128(10):849–59.
[2] Ni Q, Tan TS, Dasari GR, Hight DW. Contribution of fines to the compressive strength of mixed soils. Géotechnique 2004;54(9):561–9.
[3] Peters JF, Ernest S, Bovney IV. Percolation threshold of sand-clay binary mixtures. J Geotech and Geoenviron Eng 136. ASCE; 2010. p. 310–3.
[4] Chien LK, Oh YN. Influence of fines content and initial shear stress on dynamic properties of hydraulic reclaimed soil. Can Geotech J 2002;39:242–53.
[5] Payan M, Senetakis K, Khoshghalb A, Khalili N. Characterization of the small-strain dynamic behaviour of silty sands; contribution of silica non-plastic fines content. Soil Dyn Earthq Eng 2017;102:232–40.
[6] Salgado R, Bandini P, Karim A. Shear strength and stiffness of silty sand. J Geotech Geoenviron Eng 2000;126(5):451–62.
[7] Wichtmann T, Hernandez M, Triantafylidis T. On the influence of a non-cohesive fines content on small strain stiffness, modulus degradation and damping of quartz sand. Soil Dyn Earthq Eng 2015;69:103–14.
[8] Yang J, Liu X. Shear wave velocity and stiffness of sand: the role of non-plastic fines. Géotechnique 2016;66(6):500–14.
[9] Been K, Jefferies MG. A state parameter for sands. Géotechnique 1985;35(2):99–102.
[10] Zlatovic S, Ishihara K. On the influence of non-plastic fines on residual strength. Proc 1st Int Conf Earthq Geotech Eng 1995;1:239–44.
[11] Murthy TG, Loukidis D, Carraro JAH, Prezzi M, Salgado R. Undrained monotonic response of clean and silty sands. Géotechnique 2007;57(3):273–88.
[12] Yang J, Wei LM. Collapse of loose sand with the addition of fines: the role of particle shape. Géotechnique 2012;62(12):1111–25.
[13] Wichtmann T, Triantafyllidis T. Influence of the grain-size distribution curve of quartz sand on the small-strain shear modulus G_{max}. Geotech Geoenviron Eng 2009;135(10):1404–18.
[14] Liu X, Yang J. Shear wave velocity in sand: effect of grain shape. Géotechnique 2018;68(8):742–8. https://doi.org/10.1680/jgeot.17.T.011.
[15] Yang J, Gu XQ. Shear stiffness of granular material at small-strain: does it depend on grain size? Géotechnique 2013;63(2):165–79.
[16] Ishihara K. Soil behaviour in earthquake geotechnics. Oxford UK: Clarendon Press; 1996.

[17] Ladd RS. Preparing test specimens using under compaction. Geotech Test J 1978;1(1):16–23.
[18] Hardin BO, Black WL. Sand stiffness under various triaxial stresses. J Soil Mech Found Div 1966;92(SM2):27–42.
[19] Iwasaki T, Tatsuoka F. Effect of grain size and grading on dynamic shear moduli of sand. Soils Found 1977;17(3):19–35.
[20] Duffy J, Mindlin R. Stress-strain relations and vibrations of granular medium. J Appl Mech 1957;24:585–93.
[21] Rahman MM, Lo SR, Gnanendran CT. On equivalent granular void ratio and steady state behaviour of loose sands with fines. Can Geotech J 2008;45(10):1439–56.
[22] Rahman MM, Lo SR, Baki MAL. Equivalent granular state parameter and undrained behaviour of sand-fines mixtures. Acta Geotech 2011;6(4):183–94.
[23] Pitman TD, Robertson PK, Sego DC. Influence of fines on the collapse of loose sands. Can Geotech J 1994;31(5):728–39.
[24] Thevanayagam S. Effect of fines and confining stress on undrained shear strength of silty sands. J Geotech Geoenviron Eng 1998;124(6):479–91.
[25] Yang J, Wei LM, Dai BB. State variables for silty sands: global void ratio or skeleton void ratio? Soils Founds 2015;55(1):99–111.
[26] Sahaphol T, Miura S. Shear modulus of volcanic soils. Soil Dyn Earthq Eng 2005;25:157–65.
[27] Huang YT, Huang AB, Kuo YC, Tsai MD. A laboratory study on the undrained strength of a silty sand from Central Western Taiwan. Soil Dyn Earthq Eng 2004;24:733–43.